Validation of a simulation model for parabolic trough collectors in a high-latitude district heating system

Frej Fogelström[1], Andrea Gambardella[2], Gireesh Nair[1], Benjamin Ahlgren[1,3], Itai Danielski[1], Truong Nguyen[1]

[1] Department of Applied physics and Electronics, Umeå University, Sweden

[2] Absolicon Solar Collector AB

[3] WSP Sverige AB

Abstract

Currently, companies in the solar heating sector may choose from a wide range of tools for modelling and simulating solar thermal power. However, due to the deviant design of some collectors, conventional simulation tools may be inadequate in correctly assessing the performance of such collectors. This study aims to test and validate an in-house simulation model for T160 PTC collectors developed by the company Absolicon Solar Collector AB by comparing measured data with simulated results. A solar district heating (SDH) plant in Härnösand, Sweden featuring 192 parabolic trough collectors (PTC) is used as a case study for the validation. Operational data such as weather data, solar heat production and collector loop/ambient temperatures were collected from the facilities of Absolicon. The data was compiled and simulated using a Python model developed for the T160 collectors. The study shows an acceptable correlation between simulated and measured data during periods with high DNI where a relatively high amount of heat is delivered to the district heating. Deviations are present during periods of low DNI and can be derived from inadequate assessments of heat losses from the piping of the installation in addition to inaccurate measurement data.

Keywords: PTC collectors, Simulation, Solar District Heating, Sweden

1. Introduction

As reported by Weiss and Spörk-Dür (2023), the world-wide annual solar thermal energy yield reached 442 TWh by the end of 2022 corresponding to approximately 153 million tons of CO_2-reduction if assumed to replace oil (Weiss and Spörk-Dür, 2023). During the same year, 41 new large-scale (>350 kW_{th}) solar heating plants for district heating, residential, commercial and public buildings were commissioned. However, implementations of SDH systems in upper Nordic regions are less common. Accordingly, there is also a scarcity of measured data from such installations.

As stated by the Swedish energy company organization Energiföretagen, the DH sector has a goal of a fully decarbonized heat supply by 2030 (Rydegran, 2023). Waste incineration constitutes approximately one-fifth of supplied energy and two-thirds of the total greenhouse gas emissions in the DH sector (Naturvårdsverket, 2024.). Increasing the effectiveness or reducing the amount of waste incineration can therefore be regarded as a priority to reach the 2030 goals. DH companies in Sweden have experienced a high increase in the costs of biofuels, where the prices for pellets and wood chips significantly have increased over the past few years (Selin and Vinterbäck, 2023). With biomass constituting approximately 47% of supplied energy in the DH sector (Khodayari, 2023), the increased cost of combustibles have increased the incentives for alternative heat sources in Sweden.

DH utilities in Sweden have started exploring the possibility of solar thermal (ST) as a viable addition to the fuel mix (Bergman, 2023). Further, an ongoing investigation as part of the IEA SHC Task 68 (IEA SHC, 2024) reports good synergies between biofuel boilers and collector fields, with solar production during summer effectively replacing boilers operating on reduced loads and low efficiencies. Additionally, the study shows DH companies reduce CO_2-impact and fuel price dependency while the boilers are subjected to reduced wear and tear. Despite recognized technical readiness, a knowledge gap exists among Swedish DH companies regarding function and feasibility of SDH systems.

10.18086/eurosun.2024.07.05 Available at http://proceedings.ises.org

For detailed design, installers of solar thermal typically use commercialized simulation software's like TRNSYS (especially with the TESS library) and Modelica (Gauthier, 2024). However, these software's may be limited in correctly assessing heat production from specially designed PTC collectors at higher latitudes (Absolicon Engineering department, 2024). This study aims to validate an in-house developed simulation tool by comparing measured and simulated data from Högslätten Solar Thermal Park in the city of Härnösand, Sweden.

2. Högslätten Solar Thermal Park

Serving as a SDH demonstration site for Absolicon Solar Collectors AB, Högslätten Solar Thermal Park is situated in the city of Härnösand (62˚ N) and consists of 192 PTC collectors with the optical efficiency of 76.4%. These collectors are connected to the DH network of the city and serve as a demonstration site for DH companies and industries. The plant was commissioned during autumn 2021 with continuous measurements of weather data and heat production. The collectors consist of 8 sub-circuits containing 24 collectors each. The collectors are mounted on a 1-axis tracking system with a solar central connected to the DH network located next to the collector field. As shown by technical parameters given in Table 1, the installation covers an area of 2 940 m^2 and has under its years of operation reached an annual heat production of approximately 329 MWh. Regulators on both collector and DH side control the temperatures in the collector loop and DH network. The plant is turned off between 1st November and 28st February to avoid unnecessary wear and tear from harsh weather conditions during winter season.

Table 1: Basic technical parameters for Högslätten Solar Thermal Park.

Technical parameter	Value	Unit
Aperture area	1 056	m^2
Total area of installation	2 940	m^2
No. of collectors	192	Pcs.
Collector type	Absolicon T160 PTC	-
Collector efficiency	76.4	%
Heat carrier fluid	Water with glycol	Type
Installed thermal power	0.74	MW
Heat production (year)	329	MWh/y
Specific production (year)	445	kWh/kW/y
Global horizontal irradiation	889.4	kWh/ m^2
CO_2 saving (year)[1]	65-189	tonnes/year

[1] Nguyen et al 2024

With the installation being commissioned in early autumn 2021, only a few weeks of measurement data is available from that year. The data used in the study was therefore collected for the years 2022-2024 (exemplary day shown in Figure 1) The temperatures were all collected from sensors at the collector side, while solar heat is measured at the DH side showing heat supplied to the DH network. At present, the installation only covers a small fraction (0.21%) of the annual heat demand in the municipality.

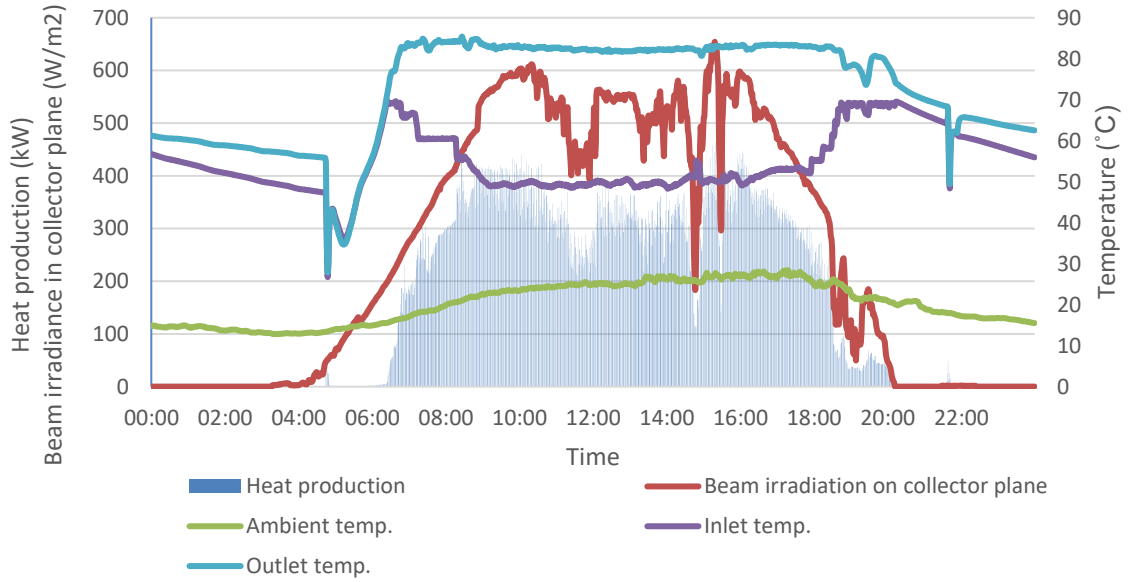

Figure 1. Measurement data during a specific day (2023-06-21) from the installation in Härnösand.

3. Methodology

3.1 Data pre-processing

Hourly measurement data on direct normal irradiation (DNI), diffuse radiation (DHI), outlet temperature, heat supplied to the DH network and ambient temperature was received from Högslätten's in-house monitoring client at the facilities of Absolicon in Härnösand. The data was divided into three separate simulation periods for 2022-2024: Simulation period 1- 1st March - 31st October 2022; Simulation period 2- 1st March - 31st October 2023; Simulation period 3 - 1st March - 6th May 2024 representing the actual periods of operation for the plant. Where inconsistent data was present during smaller time series, missing values were added using linear interpolation. Where the data was inconsistent for larger time series, missing hourly values were matched with similar data values from previous time series during the same month. Missing data points and substitution method for each of the simulation periods between 2022-2024 are presented in Table 2.

Table 2: Inconsistent measurement data and substitution method.

Interpolated		Matched from similar data series	
Date	**Time**	**Date**	**Time**
2022-07-31	06:00	2022-03-31	14:00-23:00
2022-08-31	05:00-06:00	2022-04-01	00:00-09:00
2023-03-26	02:00	2022-04-15	16:00-23:00
2023-08-30	12:00-15:00	2022-04-16	00:00-14:00
2023-10-29	02:00	2022-08-14	09:00-13:00
2024-03-31	02:00	2022-09-22	01:00-08:00

3.2. Simulation

Each data set was simulated using the in-house developed Python model for each of the simulation periods using hourly time steps. Three plot combinations were chosen for validation of simulated data; heat supplied to the DH network, outlet temperatures from the collector field and DNI/supplied heat to the DH network. Plots were created showing accumulated energy for each time step. For the outlet temperature, three separate plots during spring, summer and autumn were created for each simulation period to assess the correlation between simulated and measured data.

During the time of simulation, the U-values for the piping at Högslätten were not available why these were approximated from past projects and put in the model. Test simulations were conducted with past U-values before the value resulting in the closest mismatch between simulated and measured data was chosen (0.1 W/m, K).

3.2.1 Model function and inputs

Tilted surface radiation, row shading and collector heat output is calculated by defining functions from Mathematical Reference Compendium, TRNSYS 16: 'Solar radiation processor', 'Collector array shading' (Klein et al., n.d.) and the Solar Keymark quasi-dynamic model portrayed in ScenoCalc documentation (SolarHeatEurope, 2024). The model iterates defined functions over each time step from hourly measurement data (DNI, DHI, ambient temperature) plotting the result for simulated outlet temperatures and heat delivered to DH. The working principle of the model is shown in Figure 2.

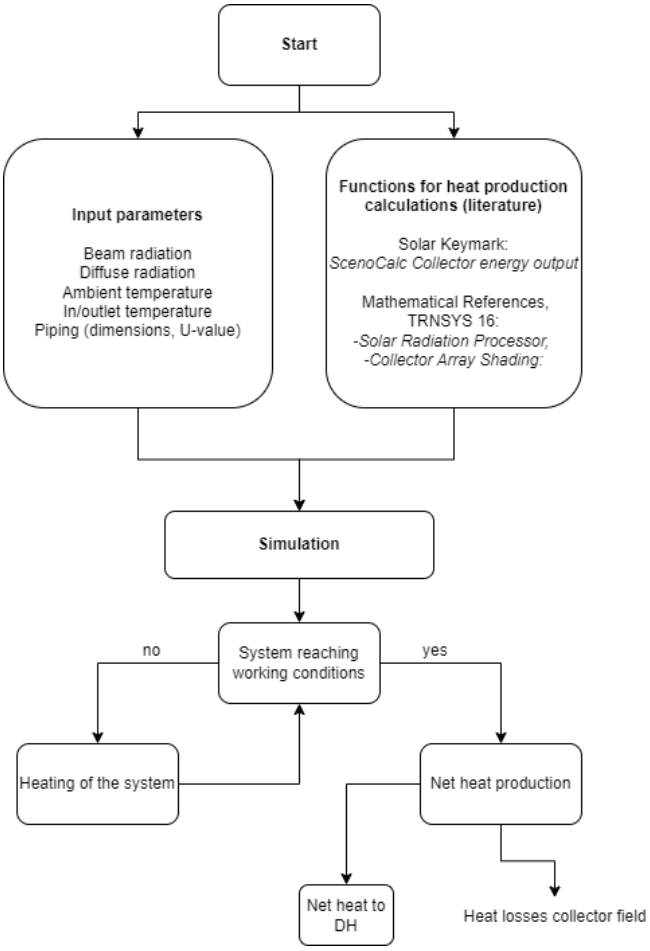

Figure 2. Schematic of the system simulation.

For fluid equations, thermodynamic relations and media properties, the Python library 'CoolProp' is used. Additionally, before heat can be supplied to the DH network, the model features a 'warm-up' function depending on ambient temperature, DNI and component properties during the start of heat production each day. The function describes the warmup of piping and system components to operational conditions until a steady state between heat carrier and system components is reached. It was created as a result from studies on actual/simulated heat production mismatches from commissioned plants and if neglected can result in a substantial shift in heat production during sunrise. Heat losses dependent on pipe dimensions as well as operational and ambient temperature are then calculated before final net heat delivered to DH is quantified and plotted.

The results are visualized in scatter plots, showing hourly accumulated heat supplied to the DH network. To further clarify the results, color mapping is used for different percentages of maximum measured DNI (0, 25, 50, 75, 100) during each simulation period showing active heat production relative measured Direct Normal Irradiance. The plots do not consider DHI as it has a negligible impact on the heat delivered from the T160 collectors. A reference line is given in each plot representing a 100% correlation between simulated and measured data. Obvious measurement

errors (simulated data 0) are marked in grey showing data points for which the input data is inconsistent/missing. To further clarify the difference between simulated and measured data, three additional plots are given showing accumulated monthly heat supplied to the DH network as well as the ratio between simulated and measured data over the time of day and relative measured DNI.

4. Results

4.1 Simulated and measured heat supplied to the DH network

The measured heat supplied to DH network was calculated to 281,42; 314,69; 34,10 MWh during Simulation period 1,2 and 3, respectively. Corresponding simulated results obtained during the same period were 206,13; 236,12; 23,87 MWh respectively, with the simulated annual results falling no more than 70% below corresponding measured values.

To give an indication on the spread of the datapoints for different values of measured DNI, a scatter plot is used (Figure 3,5,7) (light blue-blue-red-orange-yellow) representing data points of heat supplied at different levels of measured maximum DNI (0%, 25%, 50%, 75%, 100%) during each of the simulation periods. Figure 3-8 show the comparison of simulated and measured data.

4.1.1 Simulation period (1/3-31/10- 2022)

Comparison of simulated and measured data is shown in Figure 3.

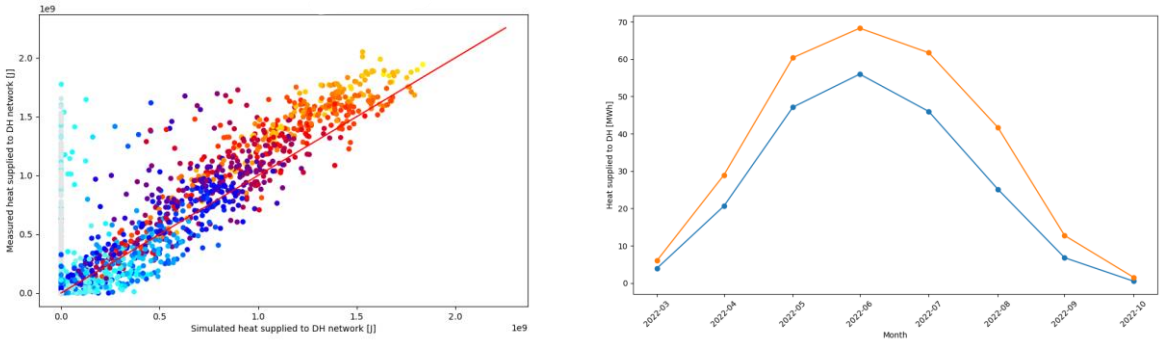

Figure 3. Simulated and measured hourly values for heat supplied to the DH network for Simulation period 1, 1/3-31/10 where the reference line (red) corresponds to a 100% match between simulated and measured data (left). Colours (light blue-red-yellow) indicate data points for different values of maximum measured DNI (0%, 25%, 50%, 75%, 100%) under the period. Measurement errors are marked in grey. Monthly comparison of simulated (blue) and measured (orange) heat supplied to the DH network (right).

The ratio simulated/measured heat supplied to the DH network relative time of day and DNI is shown in Figure 4.

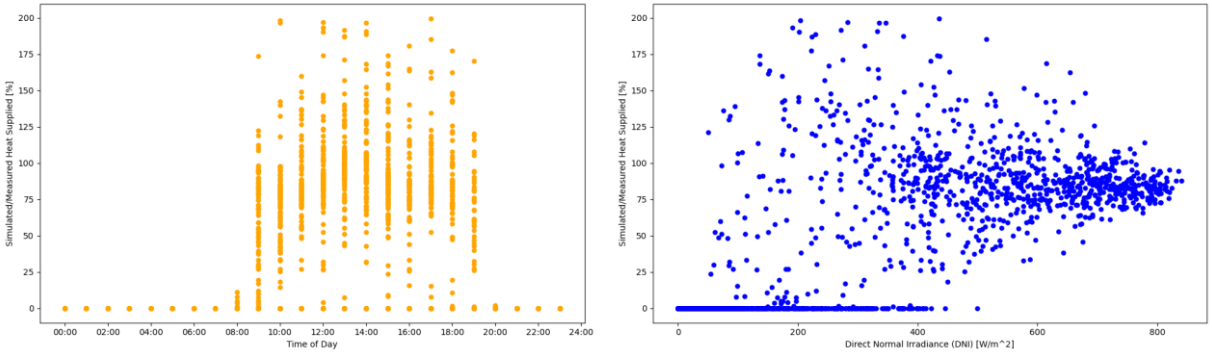

Figure 4. Simulated/measured heat (%) over the time of day (left) and relative measured DNI (right). Measurement errors occur where simulated/measured heat is zero at the bottom of the graphs.

4.1.2 Simulation period 2 (1/3-31/10- 2023)

Comparison of simulated and measured data is shown in Figure 5.

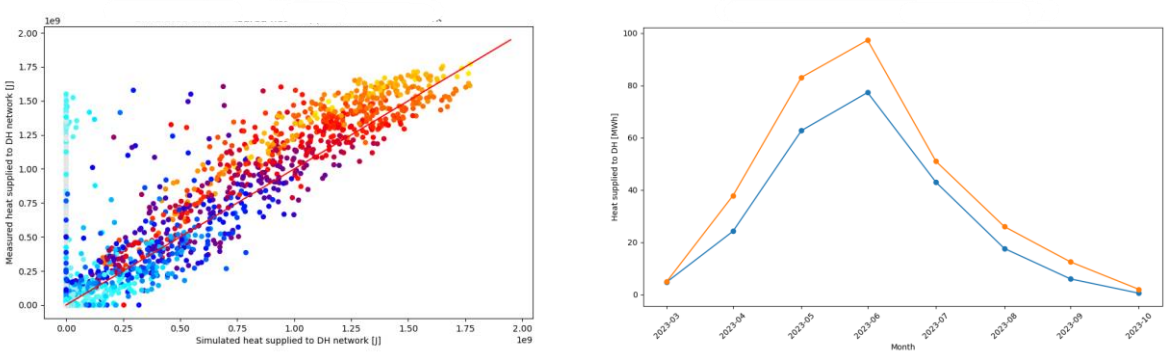

Figure 5. Simulated and measured hourly values for heat supplied to the DH network during Simulation period 2, 1/3-31/10 where the reference line (red) corresponds to a 100% match between simulated and measured data (left). Colours (light blue-red-yellow) indicate data points for different values of maximum measured DNI (0%, 25%, 50%, 75%, 100%) under the period. Measurement errors are marked in grey. Monthly comparison of simulated (blue) and measured (orange) heat supplied to the DH network (right).

The ratio simulated/measured heat supplied to the DH network relative time of day and DNI is shown in Figure 6.

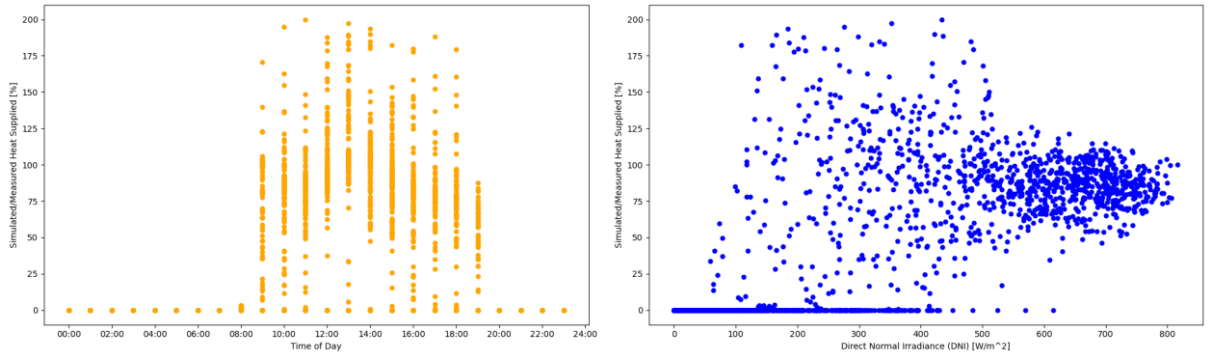

Figure 6. Simulated/measured heat (%) over the time of day (left) and relative measured DNI (right). Measurement errors occur where simulated/measured heat is zero at the bottom of the graphs.

4.1.3 Simulation period 3 (1/3-6/5- 2024)
Comparison of simulated and measured data during Simulation period 3 are shown in Figure 7.

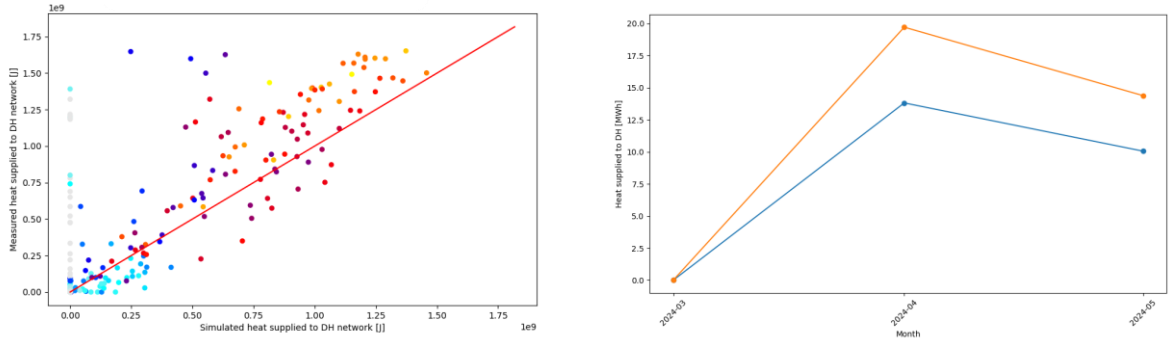

Figure 7. Simulated and measured hourly values for heat supplied to the DH network during Simulation period 3, 1/3-6/5 where the reference line (red) corresponds to a 100% match between simulated and measured data (left). Colours (light blue-red-yellow) indicate data points for different values of maximum measured DNI (0%, 25%, 50%, 75%, 100%) under the period. Measurement errors are marked in grey. Monthly simulated (blue) and measured (orange) heat supplied to the DH network (right).

The ratio simulated/measured heat supplied to the DH network relative time of day and DNI is shown in Figure 8.

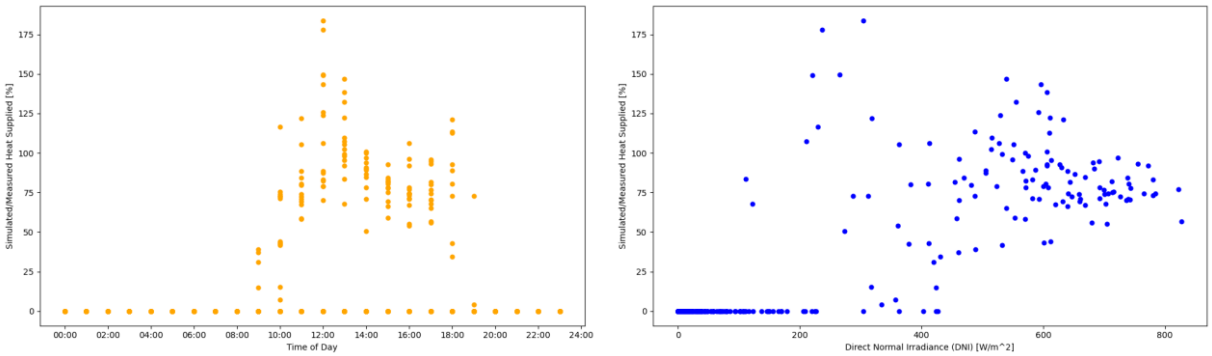

Figure 8. Simulated/measured heat (%) over the time of day (left) and relative measured DNI (right). Measurement errors occur where simulated/measured heat is zero at the bottom of the graphs.

A mismatch between simulated and measured data can be observed during simulation periods where simulated supplied heat is zero. This could be attributed to inconsistent or inaccurate input data, likely related to malfunctions or coverages of the irradiation sensors. A trend of scattered data points where measured supplied heat is higher than the simulated is present during all simulation periods. However, the colored scatterplot (Figure 3, 5, 7) reveal a trend where the deviation of data points decreases for values over 1 000 MJ.

The color mapping showing the amount of heat supplied to the DH network at different percentages of maximum DNI reveals the occurrence of lower values of heat supplied during high values of DNI. This is related to warm-up of system components, weather overcasts and thermal inertia of the system. Figure 4, 6 and 8 show the range of the mismatch between the data series decrease during the middle of the day and during periods with high DNI, correlating with the decreased deviation of data points (Figure 3, 5, 7) for high amounts of heat supplied.

4.2 Simulated and measured collector outlet temperatures

This section shows hourly collector outlet temperatures from Högslätten solar thermal park from a week during spring (April), summer (July) and autumn (October) for each of the simulation periods. The plateaus and tops in the graphs represent the operational hours of the collector field and the sinks accordingly the standby hours during nighttime.

4.2.1 Simulation period 1 (1/3-31/10- 2022)

The collector outlet temperatures during Simulation period 1 are shown in Figure 9.

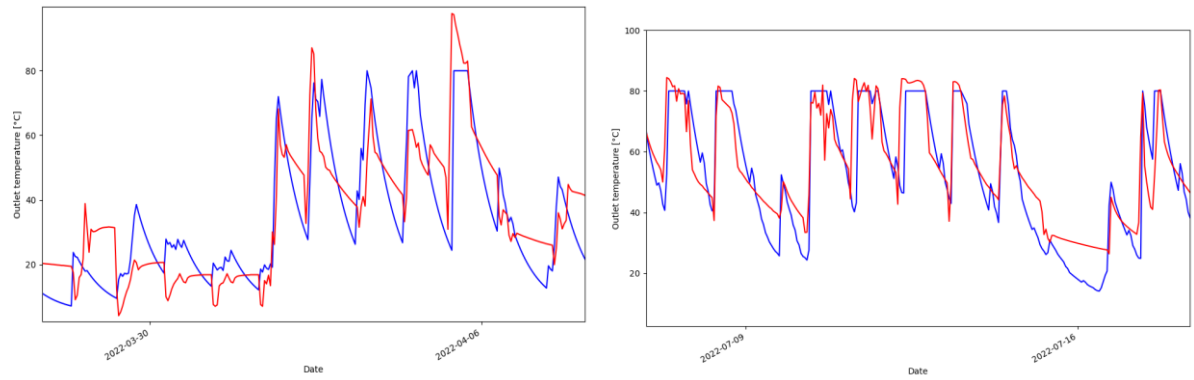

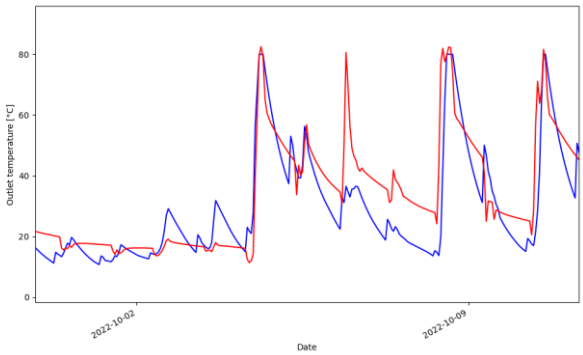

Figure 9. Simulated (blue) and measured (red) hourly outlet temperatures for April (left), July (right) and October (bottom) during Simulation period 1.

4.2.2 Simulation period 2 (1/3-31/10- 2023)
The collector outlet temperatures during Simulation period 2 are shown in Figure 10.

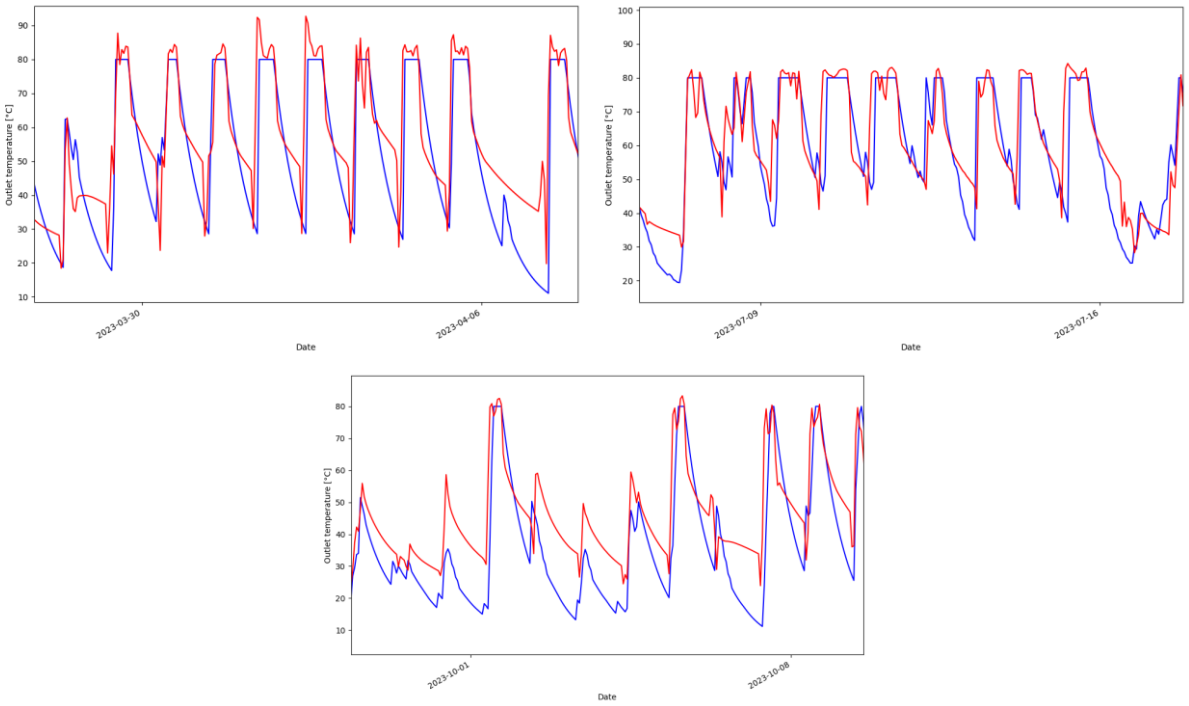

Figure 10. Simulated (blue) and measured (red) hourly outlet temperatures for April (left), July (right) and October (bottom) during Simulation period 2.

4.2.3 Simulation period 3 (1/3-6/5- 2024)
The collector outlet temperatures during Simulation period 3 are shown in Figure 11.

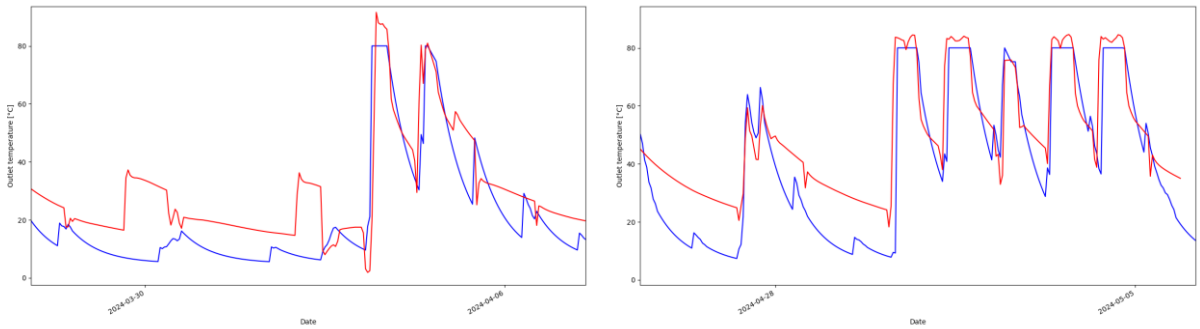

Figure 11. Simulated (blue) and measured (red) hourly outlet temperatures for April (left) and May (right) and October during Simulation period 3.

Figure 10-11 show a clearer overview of “pockets” forming between simulated and measured data in the lower temperature regions during nighttime. However, this trend disappears during operational hours in daytime where a general close correlation between simulated and measured data can be observed. The mismatch between the data series during nighttime could be related to the dissipation of heat during the installations non-commissioning hours and approximated U-values for the piping of the installation further discussed in section 5.

4.3 DNI and measured heat supplied to the DH network

To further evaluate the correlation between heat delivered to the DH network and available irradiation plots are created for each simulation period (Figure 12-13) showing measured DNI relative supplied heat to the DH network.

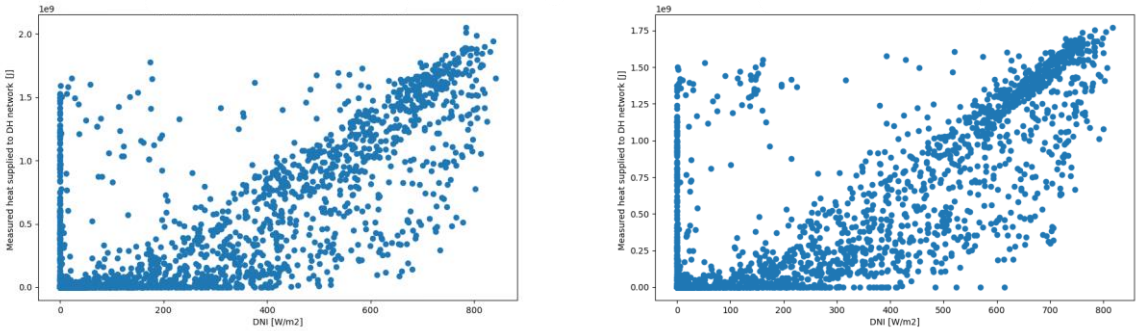

Figure 12. DNI and measured heat supplied to the DH network for Simulation period 1 (left) and 2 (right), 1/3-31/10.

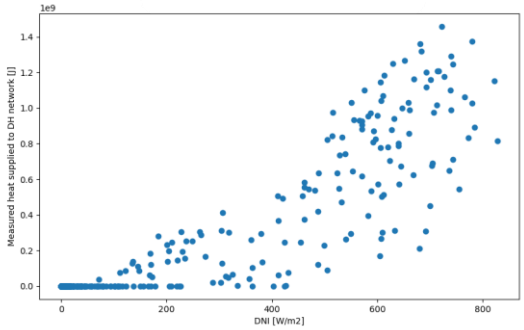

Figure 13. DNI and measured heat supplied to the DH network for Simulation period 3, 1/3-6/5.

Figure 12-13 show heat is delivered to the DH network during hours with low or no DNI and are hence measurement errors. Additionally, an accumulation of data points showing low or no measured heat for DNI between 0-400 W/m^2 can be observed. While a linear relationship between heat supplied and DNI is prominent during all simulation periods, a shift towards a trend with high DNI/low heat supplied is present during all simulation periods. The figures show all three periods have data in the complete DNI and measured heat range while featuring the same general trend and are thus comparable for analyses.

5. Discussion

5.1 Simulated and measured heat supplied to the DH network

As can be observed in Figure 3-8, data points with varying values on measured heat supplied to DH where the simulated values are zero are present during all simulation periods. A probable cause to this result is inaccurate input data used in the simulation model. For example, fluctuations and malfunctions of the irradiation sensors (bird feces, leaves, pollen etc.) at Högslätten have been reported that could contribute to incorrect measurements resulting in deviation of simulated and measured values. In addition, malfunctions on temperature sensors used to calculate heat supplied to the DH network have been reported on rare occasions.

The slight shift of data points above the reference line and mismatch of accumulated monthly data (Figure 3, 5, 7) where the measured results exceed the simulated for high values of heat supplied is affected by the defined U-value used for the piping of the solar field. During the study, U-values for the piping of Högslätten were not available and

were therefore approximated from earlier studies. In addition, simulations were carried out with varying U-values to achieve the best correlation between simulated and measured data. The magnitude of the heat losses from the piping is dependent on operational and ambient temperature and can be regarded as a dynamic variable. With the heat losses being determined from one approximated U-value during the simulations, the trend where measured values exceed the simulated results is explained by the simplification of the dynamic heat losses. Accordingly, inadequate assessments of heat losses for varying ambient and operational temperatures constitute the most prominent source of error in the simulation architecture. The monthly comparisons show an increased mismatch between the data series for months with high heat supplied, while the range of the mismatch clearly is reduced in the scatter plots during periods with high DNI/heat supplied. This is likely due to the higher number of days with heat production, resulting in "one-time" losses when the plant is cooling down and gets heated up respectively.

5.1.1 Ratio simulated/measured heat supplied to DH

The figures showing the ratio simulated/measured heat supplied to DH indicate a trend with a reduced number of outliers during high levels of DNI. Accordingly, in the case of simulated/measured heat supplied relative time of day, the same trend is present with the least number of outliers occurring during mid-day. It can therefore be concluded that the simulation model is most accurate during operational hours with high DNI. This correlates well with the results on simulated and measured outlet temperatures, where the mismatch is prominent during nighttime and negligible during daytime.

5.2 Simulated and measured collector outlet temperatures

As can be observed in Figure 9-11, there is generally a good correlation between simulated and measured collector outlet temperatures during operational hours for all simulation periods. Deviations are especially prominent during Simulation periods 2 and 3 where "pockets" are formed between simulated and measured data during non-operational hours. In most cases, the simulated data forms the pocket by assuming lower values relative the measured. With the pockets representing the outlet temperature during nighttime, the simulation model is accordingly not completely accurate during these time periods with the simulated dissipation of heat falling below the measured values.

During the initial test simulations with varying U-values (Section 3.1), the appearance of the pockets changed. However, while the pockets reduced in size for certain values, additional mismatches occurred during operational hours. Accordingly, the U-value used in the final simulations was derived from several iterations during the test phase. It can therefore be concluded that the U-values set in the model strongly affects the simulated temperatures. This is especially distinct during the first half of Simulation period 3 (Figure 11) where there is a consistent mismatch between simulated and measured data. In general, the correlation between simulated and measured data is increased during the installation's operational hours during daytime. The pockets and mismatch between simulated and measured data for low temperatures can partly be explained by the U-value used in the model being approximated for operational temperatures. To correctly assess heat losses from the pipes in the installation, convection occurring between the heat transfer fluid and the inside of the pipes in addition to ambient air and the surface of the pipes should be considered. Additional heat transfer mechanisms describing conduction through the pipes as well as heat radiation from the pipe surface to surroundings are all approximated into one U-value.

With the U-value representing all the above heat transfer mechanism during operational temperatures, it may be concluded that the increased mismatch between simulated and measured data during non-operational hours could be reduced by correctly assessing heat losses from the pipes in the collector field.

5.3 DNI and measured heat supplied to the DH network

In the case of DNI and measured heat supplied to the DH network, a trend similar to Figure 3-8 can be observed with accumulations of data points for measured heat supplied when the DNI is zero. This is a prominent source of error in the input data, where the irradiation sensors used at Högslätten could be malfunctioning. On a few occasions, bird feces or leaves have been reported to stick to the sensors further increasing the inaccuracy of the measurements.

Additional accumulations of data points can be observed close to the x-axis for values of DNI and no measured heat supplied to the DH network. This trend predominately occurs for DNI-values below 400 W/m^2. This is due to the generated heat being used to warm working parts of the installation in the mornings. Heat is supplied to the DH network when the difference between the temperature of the system components and heat carrier is reduced, enabling heat transport between the collector field and solar central. The "belly-shaped" area in the figures where low measured heat supplied and high DNI is present is related to the above phenomena, with heat supplied slowly

increasing with measured DNI as the system gradually heats up.

6. Conclusion

In this study, validation of a simulation model developed for T160 parabolic trough collectors is conducted by comparing simulated and measured data from Högslätten solar thermal park.

In the case of simulated and measured heat supplied to the DH network, deviating values mainly occur due to incorrect or inconsistent measurement data which may be attributed to occasional errors in the readings from irradiation sensors. The trend related to higher measured and lower simulated data points are most likely related to the approximation of U-values for the piping of the installation. The mismatch between simulated and measured collector outlet temperatures during standby hours in the nighttime can accordingly be derived from the same phenomena, where heat losses from the pipes vary with the temperature dependence of the U-value. With the plant cooling down during nighttime and systematically warms up during daytime, more elaborate functions are needed to assess the behaviour more accurately.

The study shows an acceptable correlation between simulated and measured data during operational hours where a relatively high amount of heat is delivered to DH. Deviating trends are consistent for all simulation periods, have the same appearance and can be derived from inaccurate measurement data or inadequate approximations of heat losses for varying operational temperatures. To further enhance the simulation model, the heat losses at varying operating and ambient temperatures need to be assessed more accurately.

The validation process facilitated Absolicon Solar Collector AB to fine tune their in-house simulation model.

7. Acknowledgments

The authors acknowledge the funding support of Absolicon Solar Collector AB, the Industrial Doctoral School of Umeå University and the Swedish Energy Agency for the projects “Soldriven fjärrvärme för hållbara städer” (project no. 50037-1) and RESILIENT Energisystem Kompetenscentrum” (project no. 52686-1).

The authors would also like to thank Ramez Shabani and Loick Bruand at Absolicon Solar Collectors AB for access to Absolicon servers and continuous support throughout the study.

8. References

Absolicon Engineering department, 2024. Absolicon HQ, Härnösand, Sweden.

Rydegran, E., 2023. Fjärrvärmens minskade koldioxidutsläpp - Energiföretagen Sverige [WWW Document]. Energiföretagen. URL https://www.energiforetagen.se/statistik/fjarrvarmestatistik/fjarrvarmens-koldioxidutslapp/ (accessed 1.10.24).

Gauthier, G., Project Manager, Plan Energi, Denmark. Personal communication 30th April 2024.

Bergman, H., Energy strategist, Härnösand Energi och Miljö, Sweden. Personal communication 6th June 2024

IEA SHC || Task 68 || Efficient Solar District Heating Systems [WWW Document], 2024. URL https://task68.iea-shc.org/ (accessed 7.3.24).

Klein, S.A., Duffie, J.A., Mitchell, J.C., Kummer, J.P., Thornton, J.W., Bradley, D.E., Arias, D.A., Beckman, W.A., Duffie, N.A., Braun, J.E., n.d. Mathematical Reference.

Naturvårdsverket, 2024. El och fjärrvärme, utsläpp av växthusgaser [WWW Document]. URL https://www.naturvardsverket.se/data-och-statistik/klimat/vaxthusgaser-utslapp-fran-el-och-fjarrvarme/ (accessed 12.21.23).

Nguyen, T., Danielski, I., Ahlgren, B., Nair, G., 2024. Effects of solar thermal energy on district heating systems: the case of parabolic trough collectors in a high latitude region. Sustainable Energy & Fuels.

Khodayari, R., 2023. Tillförd energi - Energiföretagen Sverige [WWW Document]. Energiföretagen. URL https://www.energiforetagen.se/statistik/fjarrvarmestatistik/tillford-energi/ (accessed 12.6.23).

Selin, M., Vinterbäck, J., 2023. Läget på energimarknaderna - Biodrivmedel och fasta biobränslen.

SolarHeatEurope, 2024. Description-of-ScenoCalc-v6.1.pdf [WWW Document]. Descr.--ScenoCalc-V61pdf. URL https://solarheateurope.eu/wp-content/uploads/2019/09/Description-of-ScenoCalc-v6.1.pdf (accessed 7.2.24).

Weiss, W., Spörk-Dür, M., 2023. Solar Heat Worldwide 2023. AEE- Institute for Sustainable Technologies, IEA Solar Heating and Cooling Programme, Graz, Austria.